Synchronicity of Stress Wave Propagation in Bolt Body and Anchorage Medium

Bing Sun[1], Jie-hui Xie[1] & Sheng Zeng[2,*]

[1]School of Civil Engineering, University of South China, Hengyang 421001, China
[2]School of Nuclear Resources Engineering, University of South China, (NO28, West Changsheng Road), Hengyang 421001, China
*E-mail: usczengs@126.com

Abstract. Accurate assessment of anchoring quality depends on the accuracy of assessing stress wave velocity in the anchor system. Stress wave velocity is closely related to collaborative vibration and depends on the degree of bonding between anchor body and anchorage medium. Bonding differences can be large at different ages. Based on stress wave reflection methods, non-destructive testing of anchors was performed using sensors arranged at the same cross-section of the anchor body and anchorage medium, which showed stress wave synchronization. In the early stage of filling, stress wave synchronicity was poorer between the anchor body and mortar. Therefore, the anchor should not be treated as a composite material when determining its wave velocity. Once the mortar hardens, the stress waves become more synchronous and the anchor can be regarded as a composite material. Stress wave synchronicity between the anchor body and mortar is related to mortar age and anchorage length. The anchor length required to provide stress wave synchronization between the anchor body and mortar decreases with increasing mortar age. Stress wave velocity rules were derived for different ages to provide the basis for accurately determining the stress wave velocity in the anchor.

Keywords: *anchoring quality; collaborative length; geotechnical engineering; non-destructive testing; stress wave propagation velocity; synchronization.*

1 Introduction

When anchors are applied on a large scale, the surrounding rock mass is out of control frequently in a large area due to the influence of various factors, such as on-site construction technology, operating environment and anchor quality [1]. Therefore, real-time, fast, non-destructive testing is becoming an increasingly important issue to be solved in geotechnical engineering [2-4]. Many studies have investigated improving non-destructive testing accuracy for anchorage quality [5-7]. Beard, *et al.* discussed the application of ultrasonic guided waves for non-destructive testing of anchors and developed a special vibrator [8,9]. Zou, *et al.* obtained the propagation law of low-frequency ultrasonic guided waves for different ages of concrete anchorage systems based on the transmission method [10,11]. Ming-wu, *et al.* analyzed the characteristics of the reflection phase and

Received November 15th,2016, 1st Revision January 11th, 2017, 2nd Revision April 2nd, 2017 , Accepted for publication June 14th, 2017.
 ISSN: 2337-5779, DOI: 10.5614/j.eng.technol.sci.2017.49.2.7

variation law of energy attenuation with regards to the acoustic frequency stress wave in anchorage systems [12,13] and showed that the amplitude ratio can be used to determine the anchoring state. Jian-gong, *et al.* considered the dynamic testing signal of the anchorage system and identified the quality of the surrounding rock mass [14,15]. Yi, *et al.* studied various methods of non-destructive testing for the anchor and key parameters and excitation waves [16,17]. Bing, *et al.* discussed propagation differences for the stress wave between the dynamic testing pile with low strain and the anchor based on stress wave reflection methods [18].

In practical engineering, wave velocity is an important parameter to assess anchorage quality and determine defect locations. However, since stress wave and vibration propagation in the bolts and anchorage medium is complex, it is difficult to empirically calculate wave velocity accurately. Thus, there is no accurate and effective approach to quantify the velocity. The anchor is generally regarded as a one-dimensional rod and dynamic testing theory of the pile is used to determine the stress wave velocity in the anchor as defined by Eq. (1) [19],

$$C = \sqrt{\frac{E}{\rho}}, \tag{1}$$

where C is the stress wave velocity, ρ is the density of the medium, and E is the medium's elastic modulus. The wave velocity is not only related to material properties, but also to bond stiffness at the bonding interface to a great extent. In practice, the rod does not effectively bond with the mortar in the early stage of grouting the anchor. Although the mortar will have reached a certain stiffness at this stage, the interface adhesion is still weak and stress wave propagation is significantly different to that of a composite material, where the anchor body and anchorage medium vibrate collaboratively.

From initial anchor grouting to hardening completion, the material properties and bond stiffness constantly change. Propagation of the stress wave in the anchor is also different and the wave velocity changes accordingly. The wave velocity has a direct influence on assessing anchor quality. Therefore, it is necessary to study the wave propagation of the anchor during the construction process and later usage. The changing stress wave characteristics in the wave front of the anchor medium and bolt body as well as the required coordination length for the two waves to reach the same wave front were investigated. For laboratory model testing, sensors were arranged in the same cross section but at different positions along the anchor, and non-destructive testing was performed at different ages. Thus, changing wave front characteristics with age were analyzed, and the formation and variation of composite stress wave velocity when the anchor changes into a composite material were revealed. This research provides the basis for accurately determining stress wave propagation velocity of stress wave in anchors.

2 Theoretical Analysis of Stress Wave Propagation in the Anchor

The current study was based on the wave velocity concept determining the stress wave velocity in the anchor. Pei-ji, *et al.* introduced the material dynamic response under strong impulse loading [20]. The stress wave velocity in the anchor refers to the velocity when the excited stress wave passes to the anchor. We assumed there was sufficient bonding stiffness between the bolt body and anchorage medium, i.e. the anchor was regarded as a composite material. Figure 1 shows the control volume in the anchorage section. For the case of small strain, when the stress wave propagates in the bolt the interface between the bolt body and the anchorage medium distorts in the area immediately after the wave front, since there is dynamic shear stress along the curved surface.

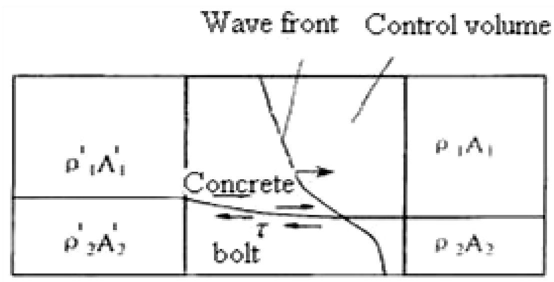

Figure 1 Control volume.

In the undisturbed region ahead of the wave front, elongation is equivalent to normal strain. Deformation is compatible between the anchorage medium and the bolt body due to bonding. Thus, from the Love kinematic conditions, we have the following Eq.(2):

$$\varepsilon_{x1} = \varepsilon_{x2} = \varepsilon = \varepsilon_x = -\frac{v}{c}, \tag{2}$$

where ε_{x1}, ε_{x2} are the normal strains of the anchorage medium and the bolt body, respectively; ε, ε_x are the elongations ahead of the wave front and normal strain, respectively; and v is the particle movement velocity.

In the quasi-static strain region, the unidirectional material equations can be expressed as in Eqs. (3) and (4):

$$\sigma_{x1} = k_1 \varepsilon_{x1} \tag{3}$$

$$\sigma_{x2} = k_2 \varepsilon_{x2} \tag{4}$$

where, σ_{x1}, σ_{x2} are the uniaxial stresses of the anchorage medium and the bolt body, respectively; and k_1, k_2, are the coefficients of equivalent stiffness of the anchorage medium and bolt body, respectively.

The coefficient of equivalent stiffness is determined by the equilibrium conditions and geometric constraints applied to the anchors rather than conditions for the anchorage medium and bolt body alone. Combining Eqs. (3) and (4), the average stress can be obtained from the average equivalent stiffness:

$$\overline{\sigma} = \sigma_{x1}\frac{A_1}{A} + \sigma_{x2}\frac{A_2}{A} = (\frac{A_1}{A}k_1 + \frac{A_2}{A}k_1)\varepsilon_x \,, \tag{5}$$

where A is the sum of the anchorage medium and bolt body volumes, A_1 and A_2, respectively; and from the conservation of momentum, as shown in Eq. (6):

$$\sigma_{x1}A_1^{'} + \sigma_{x2}A_2^{'} = cv(\rho_1 A_1 + \rho_2 A_2)\,. \tag{6}$$

If the area ratio of the anchor medium to the bolt body is $a = A_1/A_2$, then when the anchor is small, deformation state $A_1^{'} / A_1 = A_2^{'} / A_2 = 1$ and the velocity of the wave front can be obtained by combining Eqs. (2), (4), and (5) as shown in Eq. (7),

$$c^2 = \frac{A_1 k_1 + A_1 k_1}{A_1 \rho_1 + A_2 \rho_2}\,, \tag{7}$$

where the numerator represents the average equivalent stiffness derived from the status of the interface between the anchorage medium and the anchor body as well as the geometry sizes of the two media, which is different from the result obtained by the mixing method; the denominator represents the average density, which is the same as the one obtained by the mixing method.

In the velocity analysis above, the anchor was regarded as a composite material, i.e. the bonding between the anchor body and the anchorage medium assumed the ideal premise that they can vibrate totally collaboratively. However, when the adhesive force between the two tends to 0, applying an excitation wave to the bolt body will not transfer the dynamic shear stress in the distorted region to the surrounding anchorage medium effectively. Thus, in this case the anchor cannot be treated as a composite material. To explore stress wave synergy in the anchor body and anchorage medium it is necessary to consider the actual bonding situation between them.

3 Synchronization Testing on Stress Wave Propagation in the Anchor

3.1 Test Method and System

Stress wave reflection considers the impact load at the outer end of the bolt body due to the vertical vibration of a force hammer. The anchor was excited at multiple points and the output signal was measured at one single point. Figure 2 shows the test system, which comprised a dynamic signal analyzer, piezoelectric force hammer, piezoelectric acceleration sensor, signal amplifier, data collection, controller, and microcomputer processing system. The force hammer was a 2.5g LC percussion hammer (Lian Neng Company, Jiangsu, China) with charge sensitivity 3.57 PC/N. The dynamic signal analysis system was an AVANT-10 (Yi Heng Company, Hangzhou, China). To avoid frequency folding while sampling, the sampled frequency (100 kHz) was at least twice that of the highest-frequency band-limited signal. A total of 4096 samples were measured with analysis bandwidth 38.4 kHz. There were five piezoelectric acceleration transducers with frequency domains from 0.5 to 10 kHz and sensitivity 2.47 Pc/m/s^2. The measuring point locations are shown in Figure 2.

3.2 Laboratory Model

The complete anchor bolt was labeled A-1 and the defective anchor bolt A-2. The anchor dimensions were 200 mm in diameter, 2500 mm long, with a molded PVC plastic pipe. The structural scheme is shown in Figure 2.

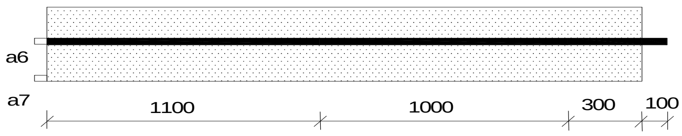

(a) Anchor A-1

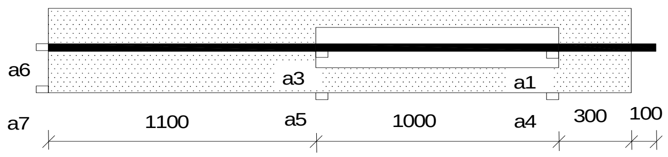

(b) Anchor A-2

Figure 2 Structural scheme and arrangement of measuring points. Note: the unit is mm, a_i (i = 1,3,4,5,6,7) is the sensor number of the corresponding measuring point.

The twisted steel used for the bolt body had a diameter of 28 mm. Cement mortar was used for the anchorage medium, with 1:2:4 water:cement:mortar composition. The construction order was that the steels were inserted first and then the mortar was poured. There was no cement mortar in the anchor defective region.

3.3 Dynamic Testing Signal Variation in the Anchor

3.3.1 Intact Anchor, A-1

The essence of non-destructive testing of an anchor is that the overall quality can be determined through vibration at a point. Between the excitation and reflection stress waves, particle vibration can be regarded as free vibration with damping under instantaneous impact load. Different measuring points have different material and vibration characteristics. Thus, it cannot be determined whether the signals from two points represent the same stress wave or not. However, if the stress waves between the steel and the mortar in the anchor system are not the same, their wave fronts are also different. They have different propagation speeds, which causes different wave front propagation times. After one reflection, a reflected fast wave front still spreads fast and a slow one still spreads slowly. This will cause the distance between the two wave fronts to increase and the time difference between the two becomes unstable, i.e. the time difference between the spreading and returning wave measured by two sensors becomes unstable.

In the early stage of grouting, the wave propagation velocity changes rapidly in the mortar but is relatively stable in the bolt body and anchor medium. Therefore, the propagation velocities of the two wave fronts are quite different and show a large time difference between the two wave fronts. With increasing age, the speed of propagation in the mortar becomes stable and the time difference between the two wave fronts reduces. Although the simplified mechanical models of two measurement points are different after hardening, their signal curves are fairly similar, since the points are in the same cross-section, forming two concentric circles respectively, and the wave front is a curve. However, due to differences in material properties, such as stiffness, propagation velocity differs, i.e. fast inside but slow outside. Therefore, the changing stress wave synchronization can be analyzed from the measurement point signals obtained by the sensors.

Figure 3 shows that with increasing age, the vibration frequency of the measured points increases. In the early stage, when the grouting has just been completed, there is little bonding between the mortar and steel and the anchor can be regarded approximately as two separate materials. As the mortar hardens, the interface bonding between the two materials gradually improves until finally the anchor can be treated as a composite material. Thus, for example, the signals from sensors a6 on the steel and sensor a7 on the mortar show time differences that decrease rapidly with aging. However, the time differences tend to a stable value rather than 0 due to innate material differences.

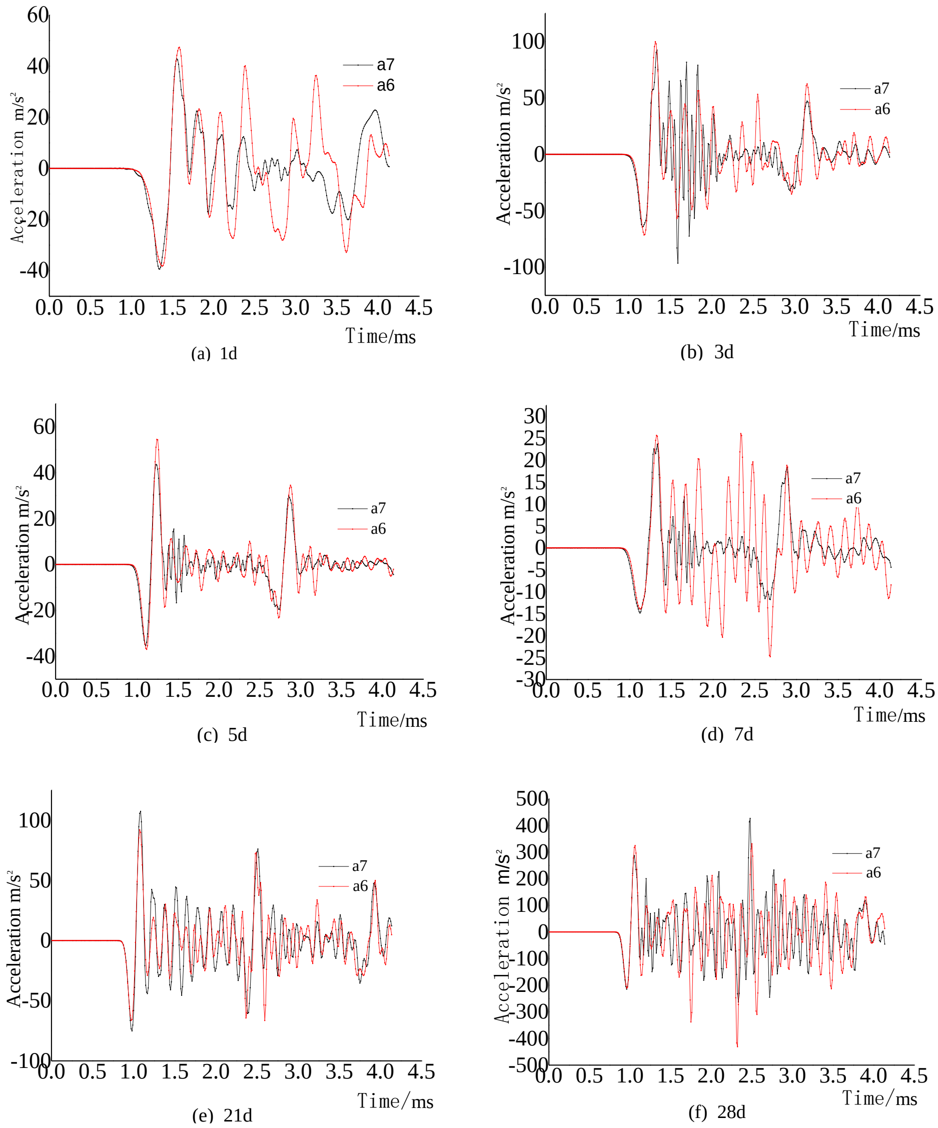

Figure 3 Dynamic testing signal of anchor A-1 at various curing times.

3.3.2 Defective Anchor, A-2

Figure 4 shows the sensor signals for the defective anchor, A-2. Similar to the A-1 case, there are time differences between sensors in the same position but on different parts before the mortar completely hardens (e.g. a6 and a7 are opposite; a3 and a5 are opposite; a1 and a4 are opposite). After the mortar hardens, the anchor can be regarded as an approximately composite material, but the time difference when the stress wave passes through the lead position of the defect is different from when it passes through the tail position of the defect.

Therefore, stress wave propagation in a defective bolt can be seen as if coming from two different materials, which separates the stress waves because in a defective region stress wave velocity in steel is larger than in mortar. Thus, the sensor on the steel at the end of the defect receives the signal first and the sensor at the same position in the mortar receives it later. If the anchor is regarded as a composite material, time differences for signals measured by the sensor at the bottom will reduce when the stress wave in the steel and mortar pass through a defective part due to the synergy of the interface. It is close to the signal of time differences for intact anchors at the bottom.

If the length before the defect meets the required length for coordination, the signal time differences for the two sensors at the beginning of the defect will be substantially the same as those at the bottom of the defective anchor. If the anchor can be treated as a composite material, after the stress wave has been reflected several times, time differences of the corresponding signals measured by sensors in a defective anchor and an intact anchor should be approximately the same.

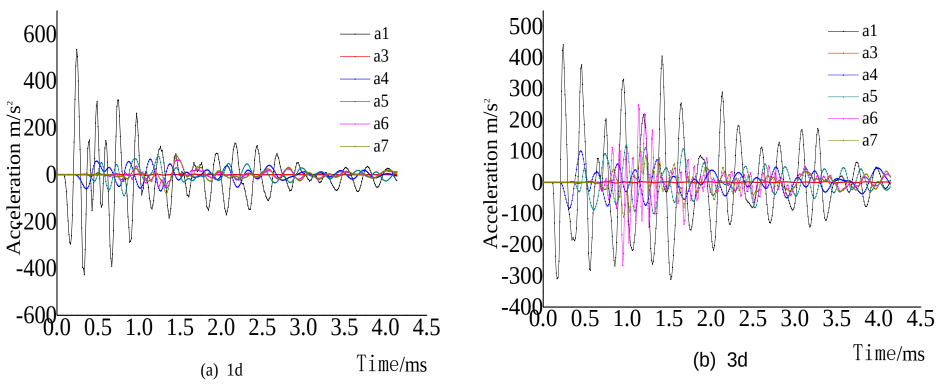

Figure 4 Dynamic testing signal of anchor A-2 at various curing times.

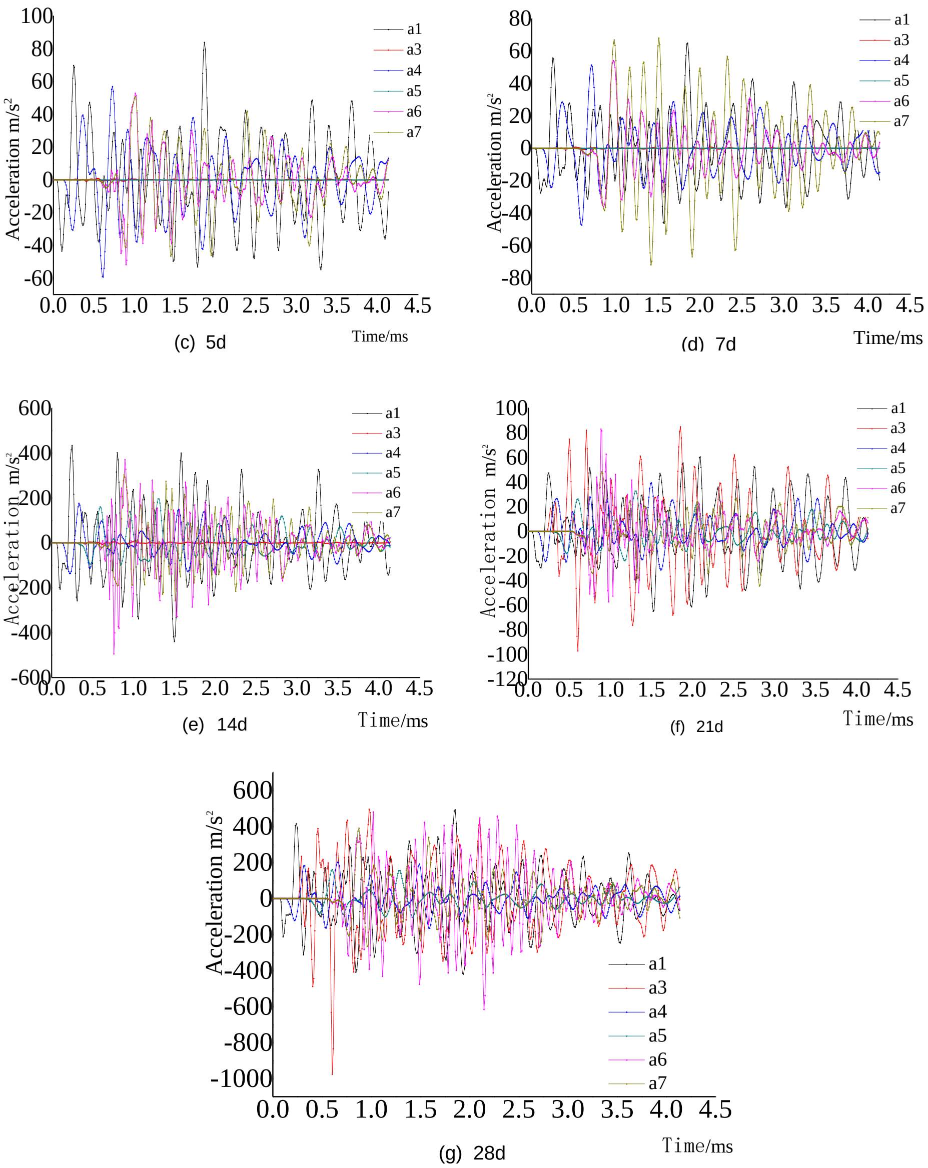

Figure 4 *continued.* Dynamic testing signal of anchor A-2 at various curing times.

3.4 Stress Wave Synchronization Variance with Aging

Figures 5 and 6 show the acceleration response curves for anchors A-1 and A-2 as the mortar ages. Section 3.3 shows that stress wave synchronization can be fully reflected by signal time differences.

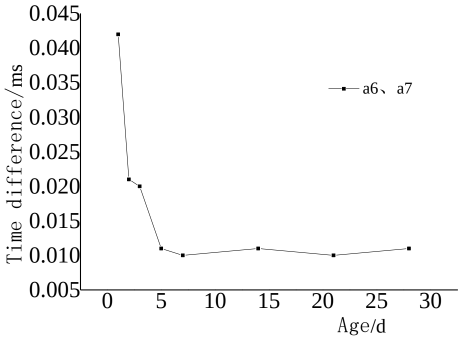

Figure 5 Time difference of two relative points on anchor A-1 at various curing times.

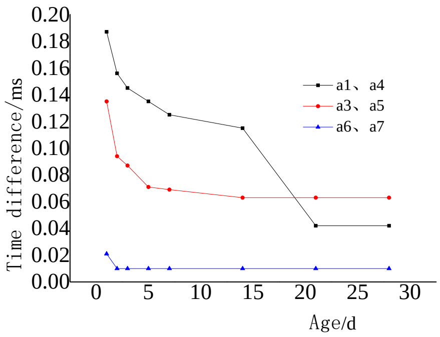

Figure 6 Time difference of two relative points on anchor A-2 at various curing times.

During the first three days, the time differences for signals measured per group of opposite sensors in A-1 and A-2 changed rapidly, and the differences between them were relatively large. After one week, the relative time differences became stable. For A-2, the time differences measured by sensors a1 and a4 differed from the time differences measured by a3 and a5 during the first two days. Whereas, once the mortar hardening was substantially completed, the time differences measured by the sensor pairs at the beginning and end of the defect tended to be stable. Thus, the anchor needs to have a certain length to ensure collaborative vibration at the bonding interface. The required length is related to the bonding stiffness. With increasing bonding stiffness, the required length to ensure stress wave collaboration between the anchor body and mortar decreases.

With increasing age, signals measured by the same sensor may also change. Since overall stiffness increases, the period shortens and frequency increases at the same time as the stress wave velocity increases. However, due to different parameters, such as the damping and stiffness of each particle at the measured points, the mechanical parameters are also different. Thus, particle vibration differs. If it is on the same wave front, when the stress wave arrives time differences between two opposing sensors are constant regardless of multiple reflections.

3.5 Required Conditions to Obtain Waveform Coordination

Figures 3 and 4 show that the measured signals for sensors a6 and a7 at the bottom can reflect anchorage quality. However, the steel signal is significantly better than the mortar signal. The mortar signal has a large vibration amplitude and small damping. Thus, although the a6 and a7 signals differ somewhat in vibration, they have consistent changes.

Because of the defect, the signals a6 and a7 for anchor A-2 vary widely at different ages. Figure 4 shows that the signals are very chaotic during the first five days and do not show the same characteristics as the detected stress wave or change tendency. However, after six days, the a6 and a7 signals show stable significant characteristics. Figure 3 shows that the integrity of A-1 is superior and the required time for waveform stabilization is relatively short.

Figures 5 and 6 show that with increasing age, the time differences measured for sensors a1 and a4 at the beginning of the defect decrease gradually but remain larger than the signals measured by sensors a6 and a7 at the bottom of the anchor for both A-1 and A-2. While a stable wave front has not yet formed at the beginning and end of the defect, it becomes closer to a stable wave front, i.e. the required length to provide stress wave coordination shortens with age. With increasing age, time differences measured by sensors a6 and a7 at the bottom of the anchors become smaller and will tend to the same wave front.

4 Conclusions

Based on stress wave reflection methods, non-destructive testing of anchors was performed by sensor pairs arranged at the same cross-section of the anchor body and anchorage medium. Time differences for arrival of the stress wave front in the anchor body and anchorage medium were evident, and different ages had different degrees of bonding and various stress wave velocities. In later usage stages, the defect meant that the required anchor length for collaborative vibration between the anchor body and mortar must also be considered.

In the early stage of grouting, stress wave synchronization between the mortar and anchor body is poor and the anchor cannot be treated as a composite material to determine stress wave velocity. Thus, stress wave synchronization can be used to determine stress wave velocity and identify anchorage quality, even in early stages of construction.

After the mortar hardens, the material physical and mechanical parameters in the anchor tend to be stable and the bonding stiffness between the bolt body and the mortar is larger. Stress wave synchronization in the bolt body and in the mortar is superior, provided the anchorage length is sufficient. The anchor can be treated as an approximately composite material to determine stress wave velocity.

The collaborative vibration of the stress wave between the anchor body and the mortar is related not only to age but also to anchorage length. A certain length is required for the stress wave of the anchor body and the mortar to reach the same wave front. With increasing age, the required anchorage length for collaboration reduces. However, further research is required to determine the specific required anchorage length for collaboration.

Acknowledgments

The authors would like to acknowledge the support of the Scientific Research Fund of the National Natural Science Foundation of China (NO.51204098), the Natural Science Foundation of Hunan Province of China (NO.11JJ6045) and the Research and Development Plan of Hunan Province of China (NO.2015SK2058-4).

References

[1] Kang, H.P., Wang, J.H. & Lin, J., *Case Studies of Rock Anchoring in Coal Mine Roadways*, Chinese Journal of Rock Mechanics and Engineering, **29**(4), pp. 649-664, 2010.

[2] Li, Y., Zhang, C.S. & Wang, C.S., *On Several Key Issues in Nondestructive Detection of Anchor Bonding Integrality*, Chinese Journal of Rock Mechanics Engineering, **27**(1), pp. 108-116, 2008.

[3] Wang, C. & Ning, J.G., *Numerical Simulation of Guided Wave Propagation in Anchored Anchors*, Chinese Journal of Rock Mechanics and Engineering, **26**(S2), pp. 3946-3953, 2007.

[4] Yang, T.G., Wu, Y.Q. & Xia, D.L., *An Analytic Method for Rock Anchor's Non-Destructive Testing Signals by Phase Deducted Method*, Journal of China Coal Society, **34**(5), pp. 629-633, 2009.

[5] Wu, R., Xu, J. & Li, C., *Stress Wave Propagation in Supporting Anchors: A Test for Anchor Support Quality*, International Journal of Ming Science and Technology, **22**(4), pp. 567-571, 2012.

[6] Neilson, R.D., Ivanovic, A. & Starkey, A.J., *Design and Dynamic Analysis of a Pneumatic Impulse Generating Device for the Non-Destructive Testing of Ground Anchorages*, Mechanical Systems and Signal Processing, **21**(6), 2007.

[7] Xue, D.C., Wu, Y. & Zhang, K., *Experimental Study and Application on Non-Destructive Testing of Anchor Axial Force in Coal Mine*, Journal of Mining & Safety Engineering, **30**(3), pp. 375-379, 2013.

[8] Beard, M.D. *Guided Wave Inspection of Embedded Cylindrical Structures*, University of London, England, 2002.

[9] Beard, M.D. & Lowe, M.J.S., *Non-Destructive Testing of Using Guided Ultrasonic Waves*, International Journal of Rock Mechanics and Mining Sciences, (40), pp. 527-536, 2003.

[10] Zou, D.H., Cui, Y. & Madenga, V., *Effects of Frequency and Grouted Length on the Behavior of Guided Ultrasonic Waves in Rock Anchors*, International Journal of Rock Mechanics & Mining Sciences, **40**, pp. 813-819, 2007.

[11] Zhang, C.S., Zou, D.H. & Madenga, V., *Numerical Simulation of Wave Propagation in Grouted Rock Anchors and the Effects of Mesh Density and Wave Frequency*, International Journal of Rock Mechanics & Mining Sciences, **43**(4), pp. 634-639, 2006.

[12] Wang, M.W., Wang, H.L. & Luo, G.Y., *Research On Non-Destructive Test of Anchoring Quality of Rock Anchors*, Journal of Engineering Geology, **7**(1), pp. 72-76, 1999.

[13] Wang, M.W. & Wang, H.L., *Nondestructive Testing of Anchoring Quality*, Chinese Journal of Rock Mechanics and Engineering, **21**(1), pp. 126-129, 2002. (In Chinese)

[14] Chen, J.G. & Zhang, Y.X., *Analysis on Characteristics of Dynamic Signal for the Anchorage System*, Chinese Journal of Geotechnical Engineering, **30**(7), pp. 1051-1057, 2008.(In Chinese)

[15] Chen, J.G., Hu, J.Q. & Zhang, Y.X., *Identification of Surrounding Rock Quality Based on Dynamic Testing Technology of Integrated Anchor*, Rock and Soil Mechanics, **30**(6), pp. 1799-1804, 2009.

[16] Li, Y., L., Hai, F. & Wang, F.C., *Nondestructive Testing of Parameters of Anchor Anchoring State and Its Application*, Chinese Journal of Rock Mechanics and Engineering, **23**(10), pp. 1741-1744, 2004.

[17] Ren, Z.M. & Li, Y., *Analysis of Detection Signal And Realization on Evaluation System of Anchor Anchoring Quality Based on Sound Wave Testing*, Journal of China Coal Society, **36**(1), pp. 191-196, 2011.

[18] Sun, B., Zeng, S. & Ding, D.X., *Research on Transmit Rules of Stress Wave with Low Strain in Dynamic Test Pile and Anchorage Anchor*, Rock and Soil Mechanics, **32**(4), pp. 1143-1148, 2011.

[19] Lei, L.Y. & Yang, C.T., *The Mathematical Models and Basic Characters of Transient Response for Dynamic Test of Pile*, Acta Geophysical Sinica, **35**(4), pp. 501-509, 1992.

[20] Zhou, P.J. & Hope Jenkins, A.K., *Material's Dynamical Response to the Strong Impulse Load*, Beijing: Science Press, 1985.